ORGANOMETALLICS

Article

Cite This: Organometallics XXXX, XXX, XXX−XXX

β-Borylalkenyl Z−E Isomerization in Rhodium-Mediated Diboration of Nonfunctionalized Internal Alkynes

Sheila G. Curto, Miguel A. Esteruelas,* Montserrat Oliván, Enrique Oñate, and Andrea Vélez

Departamento de Química Inorgánica, Instituto de Síntesis Química y Catálisis Homogénea (ISQCH), Centro de Innovación en Química Avanzada (ORFEO-CINQA), Universidad de Zaragoza-CSIC, 50009 Zaragoza, Spain

Supporting Information

ABSTRACT: The elemental steps for the preparation of (*E*)-pinBC(Me)═C(Me)Bpin (Bpin = pinacolboryl) by means of the anti addition of B_2pin_2 to 2-butyne, promoted by the boryl complex Rh(Bpin){xant(P^iPr_2)$_2$} (**1**; xant(P^iPr_2)$_2$ = 9,9-dimethyl-4,5-bis(diisopropylphosphino)xanthene), have been analyzed from a kinetic point of view, and the intermediates of the process, the β-borylalkenyl complexes Rh{(*Z*)-C(Me)═C(Me)Bpin}{xant(P^iPr_2)$_2$} (**2**) and Rh{(*E*)-C(Me)═C(Me)-Bpin}{xant(P^iPr_2)$_2$} (**3**), have been isolated and fully characterized. The key step for the formation of the diborylalkene is the transformation of **2** into **3** as a result of the *Z*−*E* isomerization of the β-borylalkenyl group, which takes place via metallacyclopropene intermediates. The isomerization is sterically controlled, and the pincer diphosphine adapts its coordination mode to the requirements of the process happening to act as κ^2-P,P. The *Z*−*E* isomerization of the β-borylalkenyl ligand of **2** is slower than the oxidative addition of the diborane to **1**. As a consequence, under catalytic conditions, the formation of the syn-addition product (*Z*)-pinBC(Me)═C(Me)Bpin is favored, although the intermediate Rh(Bpin)$_3${xant(P^iPr_2)$_2$} is much less stable than **2**.

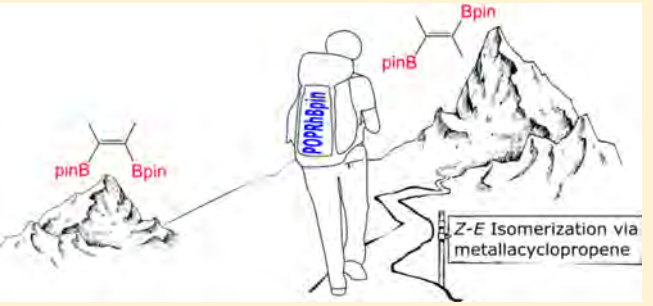

INTRODUCTION

Diborylalkenes are particularly attractive building blocks for the preparation of semiconductors based on heteroacenes[1] and bithiazole copolymers.[2] The transition-metal-catalyzed diboration of internal alkynes is without a doubt the most straightforward procedure for their synthesis.[3] Complexes of iron,[4] cobalt,[5] iridium,[6] palladium,[7] platinum,[8] copper,[9] and gold[10] have proven to catalyze the B−B addition across a C−C triple bond. The mechanism generally accepted for these reactions involves the homolytic addition of a B−B bond to the metal center of the catalyst, the insertion of the alkyne into one of the resulting M−B bonds to afford a boryl-M-{(*Z*)-β-borylalkenyl} intermediate, and finally a fast reductive elimination of the diborylalkene (Scheme 1).[3] Because all the

Scheme 1. Mechanism Generally Accepted for the Syn Addition of Diboranes to Alkynes

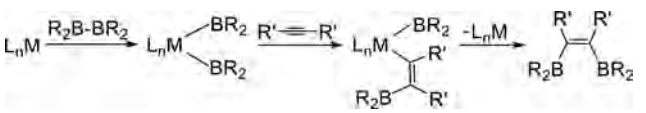

elemental reactions are concerted processes, the generated alkene systematically displays a *Z* stereochemistry in a selective manner, with a few exceptions that show mixtures of *Z* and *E* isomers.[5]

The selective formation of (*E*)-diborylalkenes is certainly challenging and has been rarely observed, being limited to functionalized substrates in non-metal-mediated processes.[11] The formation of (*E*)-diborylalkenes through metal-mediated trans addition of diboranes to internal alkynes requires the *Z*−*E* isomerization of the β-borylalkenyl group in the boryl-M-{(*Z*)-β-borylalkenyl} intermediate before the reductive elimination of the diborylalkene (Scheme 2). Thus, the study of this

Scheme 2. Steps for the Anti Addition of Diboranes to Alkynes

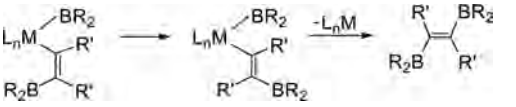

isomerization is of great importance to design the first transition-metal catalysts for the selective trans addition of diboranes to nonfunctionalized internal alkynes.

The *Z*−*E* isomerization in β-borylalkenyl groups bonded to transition metals has been observed for compounds generated from terminal alkynes in a few cases.[12] However, the scarce (*Z*)-β-borylalkenyl complexes isolated from internal substrates seem to be stable toward that isomerization.[13] In this paper, we wish to report the insertion of 2-butyne into the M−B bond of a POP-Rh-boryl complex and a kinetic study of the *Z*−*E*

Received: April 24, 2018

DOI: 10.1021/acs.organomet.8b00259
Organometallics XXXX, XXX, XXX−XXX

isomerization of the resulting β-borylalkenyl, in the context of the first rhodium-catalyzed diboration of an internal alkyne.

RESULTS AND DISCUSSION

Insertion of 2-Butyne. The complex Rh(Bpin){xant-(P^{i}Pr$_2$)$_2$} (**1**; xant(P^{i}Pr$_2$)$_2$ = 9,9-dimethyl-4,5-bis-(diisopropylphosphino)xanthene) is a notable example of a four-coordinate group 8 metal−boryl derivative,[14] which has been prepared by reaction of the monohydride RhH{xant-(P^{i}Pr$_2$)$_2$}[15] with pinacolborane (HBpin). This complex reacts with internal alkynes, as expected from its unsaturated character. The addition of 1.0 equiv of 2-butyne to pentane solutions of **1**, at room temperature, instantaneously leads to the β-borylalkenyl derivative Rh{(*Z*)-C(Me)═C(Me)Bpin}-{xant(P^{i}Pr$_2$)$_2$} (**2**), as a result of the concerted addition of the Rh−B bond of **1** across the C−C triple bond (Scheme 3).

Scheme 3. Insertion of 2-Butyne into the Rh−B Bond of 1

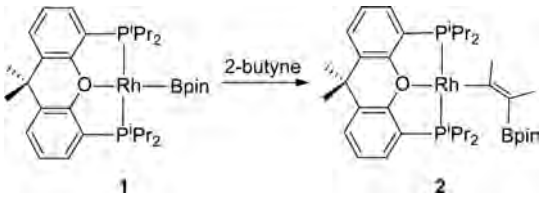

Complex **2** was isolated as a red solid in almost quantitative yield and characterized by X-ray diffraction analysis. The structure (Figure 1) proves the *Z* stereochemistry of the β-borylalkenyl group, which is disposed trans to the oxygen atom of the diphosphine (O−Rh−C(1) = 175.89(10)°). The Rh−C(1) and C(1)−C(3) distances of 1.969(3) and 1.367(4) Å, respectively, compare well with those reported for other rhodium−alkenyl complexes.[16] In agreement with the presence of this group, the ^{13}C{^{1}H} NMR spectrum in toluene-d_8, at 267 K, shows a doublet of triplets ($^1J_{C-Rh}$ = 38.9, $^2J_{C-P}$ = 12.1 Hz) at 187.1 ppm, corresponding to C(1), whereas the ^{11}B NMR spectrum contains a broad signal at 31.2 ppm due to the Bpin substituent. The Rh(POP) skeleton is T-shaped with the metal center situated in the common vertex and P(1)−Rh−P(2), P(1)−Rh−O(1), and P(2)−Rh−O(2) angles of 162.79(3), 82.00(5), and 81.56(5)°, respectively. Thus, the geometry around the rhodium atom is almost square planar with equivalent phosphines, which display a doublet with a characteristic value of 193.6 Hz for the P−Rh(I) coupling constants, at 32.8 ppm, in the ^{31}P{^{1}H} NMR spectrum. The greatest deviation from the best plane through Rh, C(1), O(1), P(1), and P(2) atoms is 0.0702 Å and involves Rh.

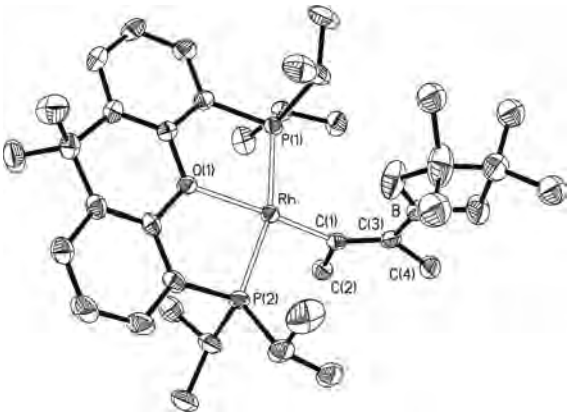

Figure 1. Molecular diagram of complex **2** (ellipsoids shown at 50% probability). All hydrogen atoms are omitted for clarity. Selected bond distances (Å) and angles (deg): Rh−P(1) = 2.2396(8), Rh−P(2) = 2.2489(8), Rh−O(1) = 2.231(2), Rh−C(1) = 1.969(3), C(1)−C(3) = 1.367(4); P(1)−Rh−P(2) = 162.79(3), O(1)−Rh−C(1) = 175.89(10), P(1)−Rh−O(1) = 82.00(5), P(2)−Rh−O(2) = 81.56(5)°.

***Z*−*E*-Isomerization.** The C−N triple bond of arylnitriles also adds to the Rh−B bond of **1**. The resulting Rh{C(aryl)═NBpin}{xant(P^{i}Pr$_2$)$_2$} species are unstable and evolve into the corresponding derivatives Rh(aryl){xant(P^{i}Pr$_2$)$_2$} as a result of the extrusion of CNBpin.[17] Complex **2** does not experience a similar reaction, releasing MeC≡CBpin. Nevertheless, it is also unstable. In toluene or pentane, it undergoes *Z*−*E* isomerization to afford Rh{(*E*)-C(Me)═C(Me)Bpin}{xant(P^{i}Pr$_2$)$_2$} (**3**), which was isolated as a red solid in 86% yield (Scheme 4).

Scheme 4. Isomerization of 2 into 3[a]

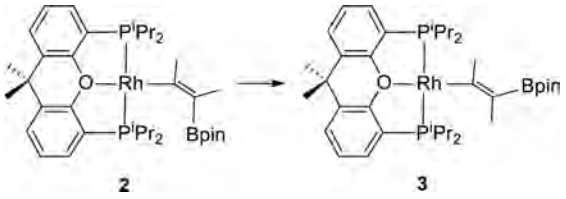

[a]Temperatures and rate constants are given in Table 1.

Complex **3** was also characterized by X-ray diffraction analysis. The structure (Figure 2) demonstrates the *E* stereochemistry of the β-borylalkenyl group and therefore the isomerization. The coordination polyhedron around the rhodium atom resembles that of **2** with O−Rh−C(1A) and P(1)−Rh−P(2) angles of 174.14(13) and 162.07(3)°, respectively. Characteristic spectroscopic features of the β-borylalkenyl ligand in benzene-d_6 are a doublet of triplets ($^1J_{C-Rh}$ = 38.2, $^2J_{C-P}$ = 11.0 Hz) at 194.8 ppm corresponding to

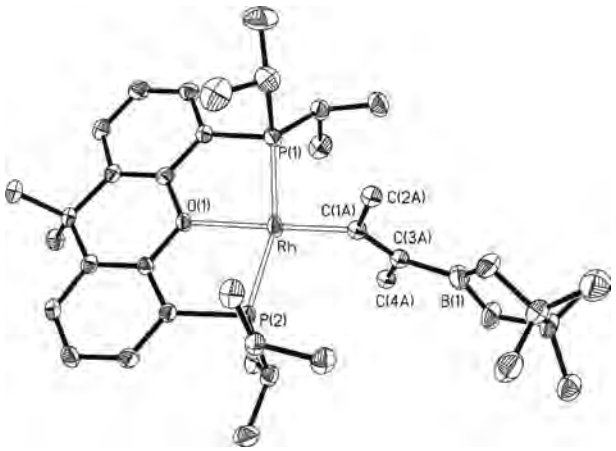

Figure 2. Molecular diagram of complex **3** (ellipsoids shown at 50% probability). All hydrogen atoms are omitted for clarity. Selected bond distances (Å) and angles (deg): Rh−P(1) = 2.2375(8), Rh−P(2) = 2.2482(8), Rh−O(1) = 2.2343(18), Rh−C(1A) = 1.997(4), C(1A)−C(3A) = 1.356(5); P(1)−Rh−P(2) = 162.07(3), O(1)−Rh−C(1A) = 174.14(13), P(1)−Rh−O(1) = 81.76(5), P(2)−Rh−O(2) = 81.57(5).

DOI: 10.1021/acs.organomet.8b00259
Organometallics XXXX, XXX, XXX−XXX

the RhC carbon atom in the $^{13}C\{^1H\}$ NMR spectrum and a broad signal at 30.6 ppm due to the Bpin substituent in the ^{11}B spectrum. The $^{31}P\{^1H\}$ NMR spectrum shows a doublet ($^1J_{P-Rh}$ = 191.0) at 34.8 ppm.

The isomerization in toluene was followed by $^{31}P\{^1H\}$ NMR spectroscopy as a function of the time between 313 and 353 K. As shown in Figure 3 for the transformation at 333 K, the

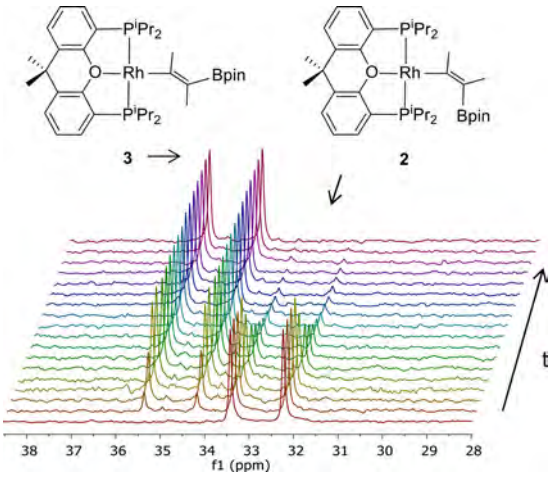

Figure 3. Stacked $^{31}P\{^1H\}$ NMR spectra (161.98 MHz, toluene-d_8, 333 K) showing the isomerization of **2** into **3** as a function of time.

decrease of **2** with the corresponding increase of **3** is an exponential function of time, in agreement with a first-order process, which fits to the expression

$$\ln \frac{[\mathbf{2}]}{[\mathbf{2}]_0} = -k_1 t \qquad (1)$$

where $[\mathbf{2}]_0$ is the initial concentration of **2** and $[\mathbf{2}]$ is the concentration at the time t. The obtained values for the rate constant k_1 in the temperature range studied are collected in Table 1. The activation parameters obtained from the Eyring

Table 1. Rate Constant k_1 (s^{-1}) for the Isomerization of 2 into 3, Calculated According to eqs 1 and 5, as a Function of Temperature (K)

temp	k_1(eq 1)	k_1(eq 5)
313	$(1.0 \pm 0.1) \times 10^{-4}$	$(7.3 \pm 0.1) \times 10^{-5}$
323	$(2.4 \pm 0.1) \times 10^{-4}$	$(2.5 \pm 0.2) \times 10^{-4}$
333	$(7.9 \pm 0.2) \times 10^{-4}$	$(6.5 \pm 0.1) \times 10^{-4}$
343	$(1.9 \pm 0.1) \times 10^{-3}$	$(1.7 \pm 0.1) \times 10^{-3}$
353	$(6.3 \pm 0.1) \times 10^{-3}$	$(4.6 \pm 0.1) \times 10^{-3}$

analysis (Figure 4) are $\Delta H^{\ddagger}$ = 21.9 ± 1.9 kcal mol^{-1} and $\Delta S^{\ddagger}$ = −7.4 ± 5 cal K^{-1} mol^{-1}, which yield a $\Delta G^{\ddagger}$ value at 298 K of 24.1 ± 3.4 kcal mol^{-1}. The slightly negative value of the activation entropy is consistent with an intramolecular process, which occurs by a geometrically highly oriented transition state.

Two approaches are generally provided to rationalize the $Z-E$ isomerization of β-substituted M−alkenyl ligands,[18] which are inspired by the early proposals of Crabtree[19] and Ojima[20] on the mechanism of the trans addition of silanes to alkynes: metallacyclopropene and zwitterionic carbene pathways. Although the isomerization via metallacyclopropene intermediates is the most accepted, it is unclear how the process occurs. To gain mechanistic insight about the isomerization of **2** into **3**,

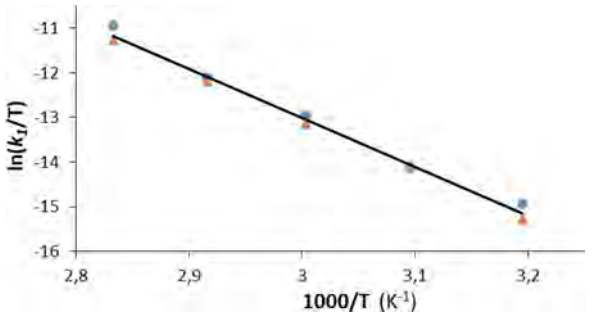

Figure 4. Eyring plot for the isomerization of **2** into **3**: (blue ●) k_1 values calculated according to eq 1; (orange ▲) k_1 values calculated according to eq 5 in the presence of B_2pin_2.

we have carried out DFT calculations (B3LYP(GD3)//SDD(f)/6-31G**). The changes in free energy (ΔG) were tabulated in toluene at room temperature. Figure 5 summarizes the energy profile of the transformation, whereas Figure S3 gives views of the structures of intermediates and transition states.

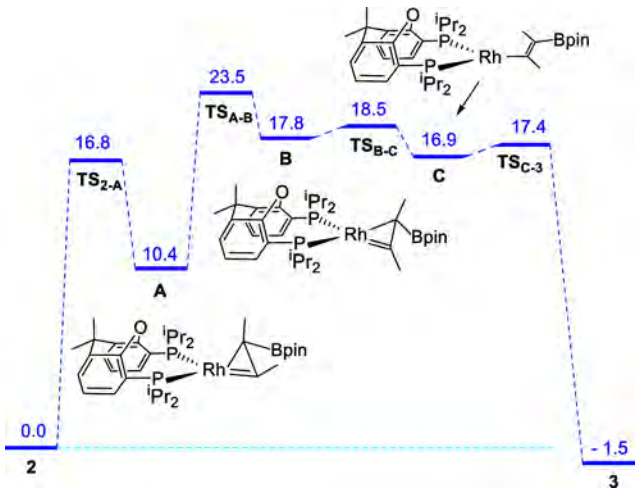

Figure 5. Energy profile (ΔG, toluene, room temperature) for the isomerization of **2** into **3**.

The isomerization takes place through intermediates **A**−**C**, which lie 10.4, 17.8, and 16.9 kcal·mol^{-1} above **2**. The coordination of the C_β atom of the borylalkenyl ligand of **2** to the rhodium atom results in the release of the oxygen atom of the diphosphine, which happens to act as κ^2-P,P. The process occurs in one step with an activation energy of 16.8 kcal mol^{-1}. The ability of xantphos-type diphosphines, including those substituted with alkyl groups,[21] to adapt their coordination mode to the requirements of the reactions has been previously demonstrated, in particular by Weller's group.[22] The formation of the rhodacyclopropene **A** increases the steric hindrance between the phosphine and the borylalkenyl substituents. As a consequence, this intermediate shows a noticeable distortion of the coordination plane toward a tetrahedral disposition, which gives rise to a dihedral angle between the planes PRhP and CRhC of 44.6°. The transformation of **A** into **B** is also a one-stage process, which involves a clockwise rotation of 96° of the C−C bond of the metallacycle with regard to an ideal coordination plane. The rotation generates a strong steric hindrance between the methyl group attached to the C(sp^2)

DOI: 10.1021/acs.organomet.8b00259
Organometallics XXXX, XXX, XXX−XXX

atom and the substituents of the diphosphine, which gives rise to a pivoting of 90° of the former with regard to the C−C bond. The motion reverses the relative disposition of the methyl substituents of the rhodacyclopropene. The transformation occurs through the transition state $\mathbf{TS_{A\text{-}B}}$ with an activation energy of 23.5 kcal mol^{-1}. This value allows the calculation of activation enthalpy and activation entropy values of 22.7 kcal mol^{-1} and −2.8 cal K^{-1} mol^{-1}, respectively, which compare well with those obtained from the Eyring analysis shown in Figure 4. In $\mathbf{TS_{A\text{-}B}}$, the coordination around the rhodium atom is almost square planar; the dihedral angle between the PRhP and CRhC planes is 2.09°. Once the new metallacycle has been formed, the rhodium center dissociates the disubstituted carbon atom. The dissociation has a very low activation energy of 0.7 kcal mol^{-1}, and the resulting three-coordinate intermediate **C** is 0.9 kcal mol^{-1} more stable than **B**. The destabilization generated by the reduction in the coordination number is compensated by the decrease of the steric hindrance. Intermediate **C** is the β-borylalkenyl counterpart of the three-coordinate monohydride RhH{κ^2-*P*,*P*-xant-(P^{i}Pr$_2$)$_2$}, which has been proposed as the key species for the ammonia−borane dehydrogenation catalyzed by the square-planar monohydride RhH{xant(P^{i}Pr$_2$)$_2$}.[21b] The coordination of the oxygen atom of the diphosphine through $\mathbf{TS_{C\text{-}3}}$, with an activation energy of 0.5 kcal mol^{-1}, affords **3**, which is 1.5 kcal mol^{-1} more stable than **2**.

DFT calculations do not support a zwitterionic carbene pathway for the isomerization of **2** into **3**. The structure resulting from a 90° rotation of the pinBCMe group with regard to the C$_\alpha$−C$_\beta$ bond of the β-borylalkenyl ligand of **2** collapses into **A**.

Reaction of 3 with B_2pin_2. Complex **3** reacts with B_2pin_2 in toluene to afford (*E*)-pinBC(Me)═C(Me)Bpin and regenerate **1** (Scheme 5). The transformation was followed

Scheme 5. Reaction of 3 with B_2pin_2

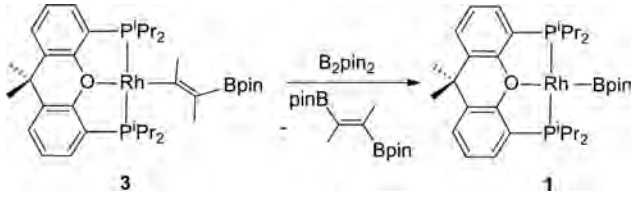

3 1

by ^{31}P{^{1}H} NMR spectroscopy in the temperature range 313−353 K, for concentrations of B_2pin_2 between 1.64 and 2.95 M, starting from a concentration of **3** of 0.033 M. Under these conditions, the decrease of **3** with the corresponding increase of **1** is an exponential function of the time, in agreement with a pseudo-first-order process. Thus, the rate constant k_{obs} for each concentration of B_2pin_2 employed and each temperature was calculated by means of the graphical representation (Figure 6) of the expression

$$\ln \frac{[\mathbf{3}]}{[\mathbf{3}]_0} = -k_{obs}t \qquad (2)$$

The plot of ln(d[**3**]/d*t*) versus ln[B_2pin_2] yields a straight line of slope 1.02 (Figure S1) demonstrating that the reaction is also first order in B_2pin_2 concentration. Therefore, the rate law is

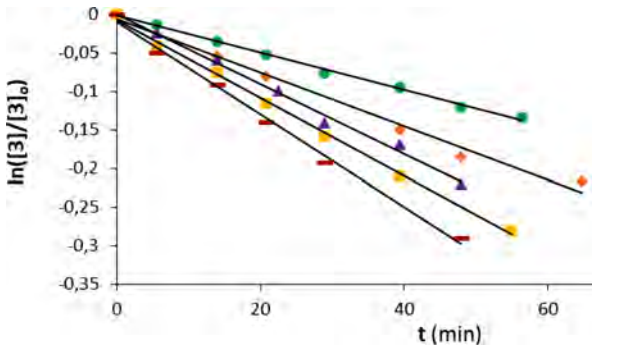

Figure 6. Graphical representation of eq 2 for the different concentrations of B_2pin_2 employed at 333 K. (green ●) 1.64 M; (orange ◆) 1.97 M; (purple ▲) 2.30 M; (yellow ■) 2.62 M; (red −) 2.95 M.

$$\frac{d[\mathbf{2}]}{dt} = -\frac{d[\mathbf{3}]}{dt} = k_3[\mathbf{3}][B_2pin_2] \qquad (3)$$

and

$$k_3[B_2pin_2] = k_{obs} \qquad (4)$$

A plot of k_{obs} versus B_2pin_2 (Figure 7) provides the rate constant k_3 for a given temperature. The values obtained in the

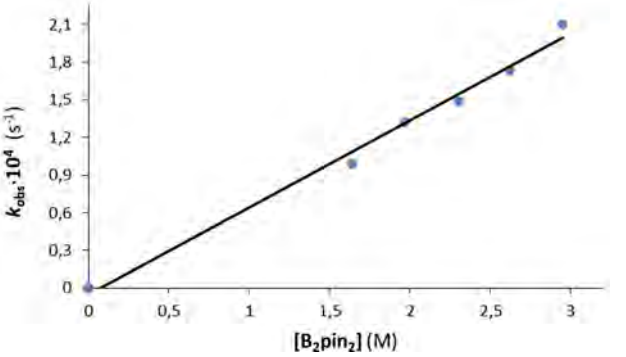

Figure 7. Plot of k_{obs} versus B_2pin_2 concentration for the reaction of complex **3** with the diborane at 333 K.

temperature range studied are given in Table 2. The activation parameters calculated from the Eyring analysis (Figure 8) are $\Delta H^{\ddagger}$ = 13.2 ± 2.2 kcal mol^{-1} and $\Delta S^{\ddagger}$ = −37.9 ± 6.6 cal K^{-1} mol^{-1}, which yield a $\Delta G^{\ddagger}$ value at 298 K of 24.5 ± 4.2 kcal mol^{-1}. The significantly negative value of the activation entropy is consistent with a σ-bond metathesis between the B−B bond of the diborane and the Rh−C bond of **3**, which occurs in a concerted fashion through a geometrically highly oriented four-centered four-electron transition state, which avoids the oxidative addition of the B−B bond to the metal center and the subsequent reductive elimination of the diborylalkene.[23]

The insertion of the alkyne into the Rh−B bond of **1** (Scheme 3), the isomerization of **2** into **3** (Scheme 4), and the reaction of the latter with the diborane (Scheme 5) form a cycle for the first metal-mediated anti diboration of a non-functionalized internal alkyne, where the *Z*−*E* isomerization of the β-borylalkenyl group, in particular the transformation of the syn metallacyclopropene **A** into the anti isomer **B**, and the reaction of the *E* isomer **3** with B_2pin_2 have similar activation energies (Scheme 6). In contrast to **3**, the (*Z*)-β-borylalkenyl isomer **2** does not react with the diborane. Between 313 and

DOI: 10.1021/acs.organomet.8b00259
Organometallics XXXX, XXX, XXX−XXX

Table 2. Concentrations (M) and Rate Constants k_{obs} (s^{-1}) for the Formation of (*E*)-pinBC(Me)=C(Me)Bpin, Starting from 3 and 2, and k_3 (M^{-1} s^{-1}) as a Function of the Temperature (K)

T	$[3]_0$	$[2]_0$	$[B_2pin_2]$	k_{obs}(eq 2)	k_{obs}(eq 7)	k_3
313	0.033		2.30	$(4.2 \pm 0.7) \times 10^{-5}$		$(1.8 \pm 0.4) \times 10^{-5}$
313		0.033	2.30		$(4.5 \pm 0.2) \times 10^{-5}$	$(2.0 \pm 0.1) \times 10^{-5}$
323	0.033		2.30	$(9.1 \pm 1.3) \times 10^{-5}$		$(4.0 \pm 0.6) \times 10^{-5}$
323		0.033	2.30		$(7.7 \pm 0.5) \times 10^{-5}$	$(3.4 \pm 0.3) \times 10^{-5}$
333	0.033		1.64	$(9.9 \pm 0.1) \times 10^{-5}$		$(6.2 \pm 0.1) \times 10^{-5}$
333	0.033		1.97	$(1.3 \pm 0.3) \times 10^{-4}$		$(6.6 \pm 0.2) \times 10^{-5}$
333	0.033		2.30	$(1.5 \pm 0.1) \times 10^{-4}$		$(6.5 \pm 0.1) \times 10^{-5}$
333		0.033	2.30		$(2.1 \pm 0.4) \times 10^{-4}$	$(9.1 \pm 0.2) \times 10^{-5}$
333	0.033		2.62	$(1.7 \pm 0.1) \times 10^{-4}$		$(6.5 \pm 0.1) \times 10^{-5}$
333	0.033		2.95	$(2.2 \pm 0.1) \times 10^{-4}$		$(7.4 \pm 0.1) \times 10^{-5}$
343	0.033		2.30	$(3.2 \pm 0.1) \times 10^{-4}$		$(1.4 \pm 0.1) \times 10^{-4}$
343		0.033	2.30		$(3.7 \pm 0.1) \times 10^{-4}$	$(1.6 \pm 0.1) \times 10^{-4}$
353	0.033		2.30	$(5.3 \pm 0.1) \times 10^{-4}$		$(2.3 \pm 0.1) \times 10^{-4}$
353		0.033	2.30		$(4.8 \pm 0.1) \times 10^{-4}$	$(2.1 \pm 0.1) \times 10^{-4}$

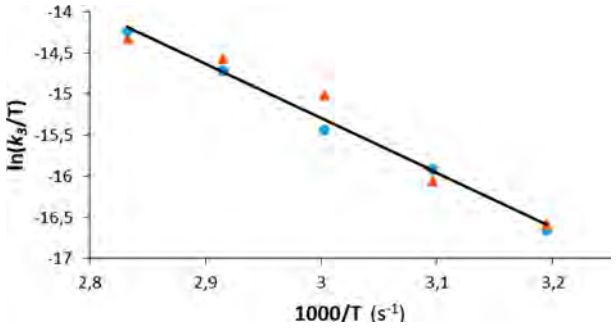

Figure 8. Eyring plot for the reaction of **3** with B_2pin_2: (blue ●) starting from **3**; (orange ▲) starting from **2**.

Scheme 6. Stoichiometric Anti Addition of B_2pin_2 to 2-Butyne

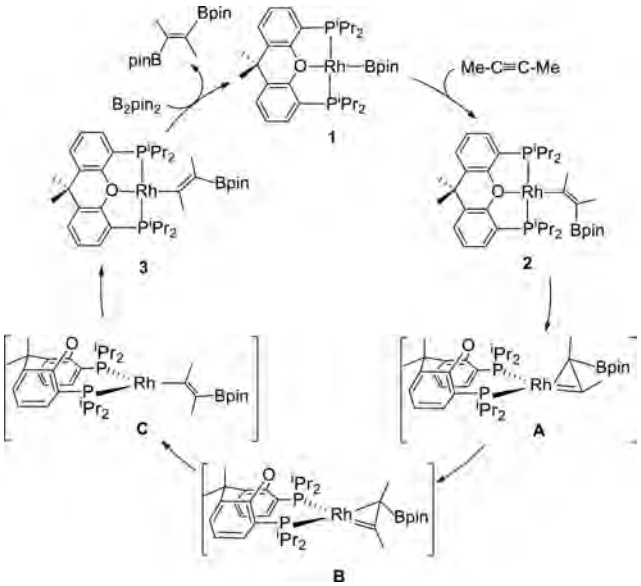

353 K, the treatment of 0.033 M of **2** with 2.30 M of B_2pin_2, in toluene-d_8 faithfully reproduces the sequence of events collected in Scheme 6. Figure 9 shows the $^{31}P\{^1H\}$ spectrum of the reaction mixture, as a function of the time, at 333 K. The dependence of the amounts of **2**, **3**, and **1** with time (Figure 10) is as expected for two consecutive irreversible reactions and

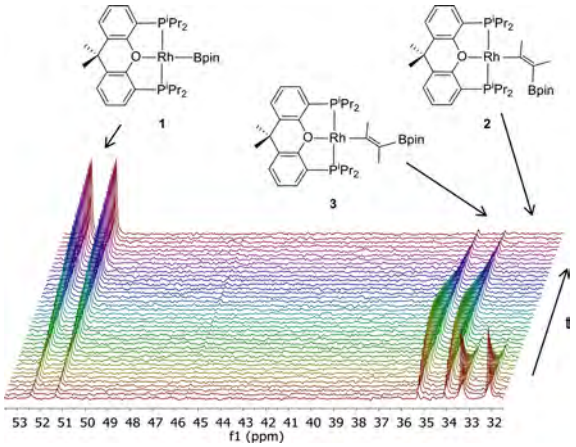

Figure 9. Stacked $^{31}P\{^1H\}$ NMR spectra (161.98 MHz, toluene-d_8, 333 K) showing the course of the reaction of **2** with B_2pin_2.

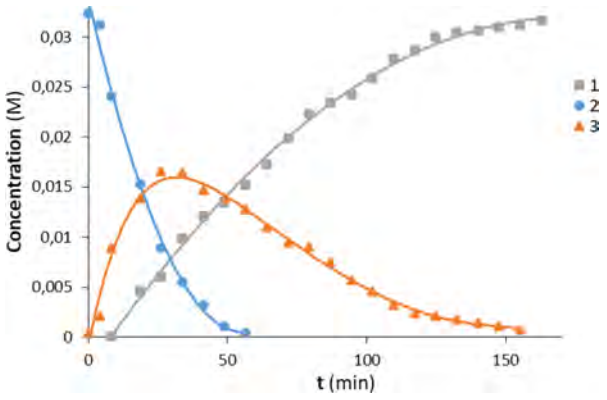

Figure 10. Composition of the mixture as a function of time for the reaction of 0.033 M of **2** with 2.30 M of B_2pin_2 at 333 K.

fits to eqs 5–7, respectively.[24] The rate constants k_1 and k_3 (via eq 4) obtained from these expressions (Tables 1 and 2, respectively) fit to the same Eyring analysis as those obtained from eqs 1 and 4 (through eq 2), as is shown in Figures 4 and 8.

$$[\mathbf{2}] = [\mathbf{2}]_0 e^{-k_1 t} \quad (5)$$

DOI: 10.1021/acs.organomet.8b00259
Organometallics XXXX, XXX, XXX−XXX

$$[\mathbf{3}] = \frac{[\mathbf{2}]_0 k_1}{k_{obs} - k_1}[e^{-k_1 t} - e^{-k_{obs} t}] \quad (6)$$

$$[\mathbf{1}] = [\mathbf{2}]_0 + \frac{[\mathbf{2}]_0}{k_1 - k_{obs}}[k_{obs} e^{-k_1 t} - k_1 e^{-k_{obs} t}] \quad (7)$$

Catalytic Addition of B_2pin_2 to 2-Butyne. Complex **1** catalyzes the addition of B_2pin_2 to 2-butyne. However, the product formed is the (*Z*)-diborylalkene. The reaction was performed in *n*-octane at 70 °C, under argon, using 5 mol % of catalyst and 0.2 M of B_2pin_2 and alkyne. Under these conditions (*Z*)-pinBC(Me)=C(Me)Bpin was selectively formed in 75% yield after 24 h (Scheme 7). Its stereochemistry was confirmed by X-ray diffraction analysis (see Figure S2).

Scheme 7. Addition of B_2pin_2 to 2-Butyne Catalyzed by 1

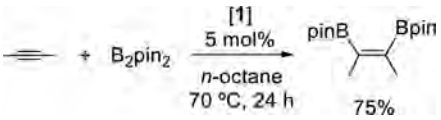

The exclusive formation of the product resulting from the syn addition of the diborane to the C−C triple bond of the alkyne indicates that the cycle shown in Scheme 6 (alkyne route) does not play any role in the catalysis. The addition of B_2pin_2 to **1** should be therefore the first step of the catalytic process, which could take place through the cycle shown in Scheme 8 (diborane route). To gain insight into the nature of

Scheme 8. Catalytic Syn Addition of B_2pin_2 to 2-Butyne

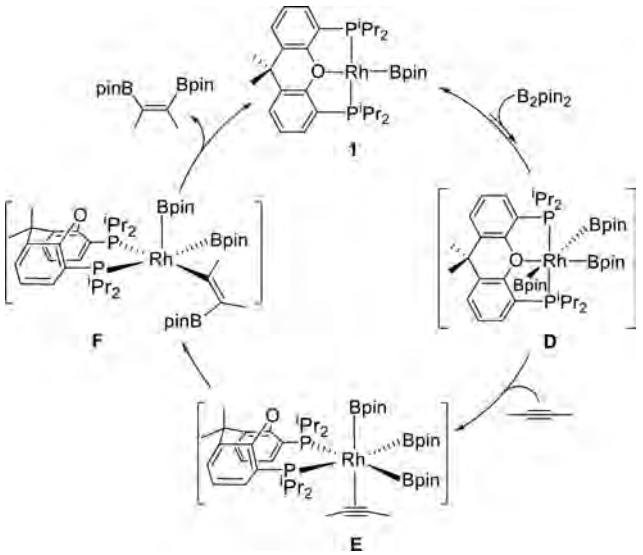

the key intermediates and the kinetic or thermodynamic preference of this route, we analyzed the addition of 25 equiv of B_2pin_2 to toluene solutions of **1**, by $^{31}P\{^1H\}$ NMR spectroscopy, between 298 and 193 K. Although changes in the spectrum of **1** were not observed in this range, the formation of intermediate Rh(Bpin)$_3${xant(P^{i}Pr$_2$)$_2$} (**D**) cannot be discarded, since it could be kinetically favored under the catalytic conditions, in spite of its low stability. In fact, the diborane route is kinetically favored and the formation of the syn addition product takes place via **D**. In agreement with this, we have observed that the $^{31}P\{^1H\}$ NMR spectrum of the solution resulting from the addition of 2 equiv of B_2cat_2 to a toluene-d_8 solution of **1** shows after 5 min, at room temperature, the characteristic resonance of Rh(Bcat){xant(P^{i}Pr$_2$)$_2$} (**4**; $\delta_{^{31}P}$ 54.5, $^1J_{P-Rh}$ = 159.9 Hz)[14] along with a broad doublet ($\delta_{^{31}P}$ 31.5, $^1J_{P-Rh}$ = 78.1 Hz) which could correspond to the rhodium(III) derivative Rh(Bpin)(Bcat)$_2${xant(P^{i}Pr$_2$)$_2$} (**5**), key intermediate for the Bpin/Bcat exchange (Scheme 9). At 333 K, the rhodium(I) complex **4** is the only detected species in the spectrum, whereas the Rh(I):Rh(III) molar ratio is 26:74 at 243 K (Figure 11). The $^{11}B\{^1H\}$ NMR spectrum at room

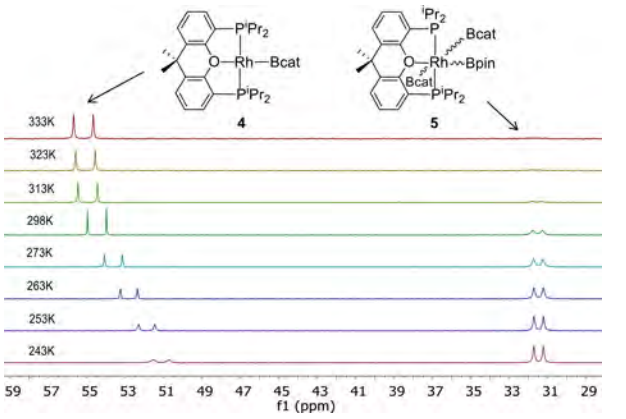

Figure 11. Stacked $^{31}P\{^1H\}$ NMR spectra (161.98 MHz, toluene-d_8) showing the products of the reaction of **1** with B_2cat_2 as a function of the temperature.

temperature consistently contains a broad resonance at 31.2 ppm, which can be assigned to the unsymmetrical diborane pinB-Bcat.[25] The broadening of the resonance corresponding to **5** by an increase in the temperature could be due to a dynamic process involving the dissociation of the diphosphine oxygen atom. In this context, it should be noted that **5** and **D** are saturated species and that both the reductive elimination of pinB-Bcat to give **4** and the coordination of the alkyne (**E**) to afford **F**, by insertion of the C−C triple bond into one of the Rh−B bonds, require the oxygen dissociation. The lower steric requirement of Bcat with regard to Bpin could explain why **5** is more stable than **D**. Electronic reasons do not appear to be relevant. Although the Bcat group is a better π-acceptor ligand than Bpin,[26] the basicity of the rhodium(III) center is very poor.[27]

Scheme 9. Reaction of Complex 1 with B_2cat_2

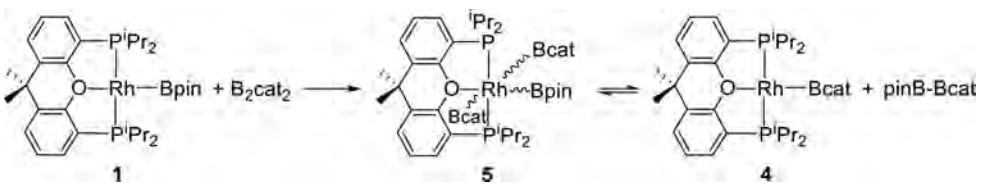

DOI: 10.1021/acs.organomet.8b00259
Organometallics XXXX, XXX, XXX−XXX

CONCLUDING REMARKS

Our results reveal that the formation of (*E*)-diborylalkenes, by metal-mediated addition of diboranes to nonfunctionalized internal alkynes, occurs when the *Z*−*E* isomerization of the *β*-borylakenyl ligand, resulting from the alkyne insertion into a M−B bond, is kinetically favored with regard to the oxidative addition of the B−B bond of the diborane, since the alkyne insertion and the reductive elimination of the diborylalkene from a boryl−metal−(*β*-borylalkenyl) intermediate are very fast steps. The isomerization of the *β*-borylalkenyl group is sterically controlled, the congestion around the metal center being the main factor to promote it. The oxidative addition of the diborane to the metal center is both sterically and electronically controlled. From a steric point of view, the congestion around the metal center prevents the approach of the diborane, whereas it destabilizes the oxidized species. Nucleophilic metal centers increase the oxidative addition rate and stabilize the oxidized species, while electrophilic metal centers produce the opposite effect. According to this, three items should be taken into account in order to design metal catalysts for the anti diboration of nonfunctionalized internal alkynes.

(i) The catalyst should have only one boryl ligand, since the reductive elimination of the diborylalkene is fast.

(ii) Ligands and diboranes with marked steric hindrance should be used, because the steric congestion around the metal center favors the *Z*−*E* isomerization of the *β*-borylalkenyl group while it prevents the oxidative addition of the diborane.

(iii) Electrophilic metal centers should be employed, because this class of metals prevents the oxidative addition. Furthermore, they should favor the *σ*-bond metathesis between the B−B bond of the diborane and the M−C bond of the *β*-borylalkenyl intermediate, which is sterically controlled as the *Z*−*E* isomerization of the *β*-borylalkenyl group.

In conclusion, the formation of (*E*)-diborylalkenes by catalytic anti diboration of nonfunctionalized internal alkynes needs a catalyst with only one M−boryl bond, which does not undergo oxidative addition of diboranes, and requires the *Z*−*E* isomerization of the *β*-borylalkenyl group, generated from the alkyne insertion into the M−B bond, and a *σ*-bond metathesis between the B−B bond of the diborane and the M−C bond of the (*E*)-*β*-borylalkenyl intermediate, resulting from the isomerization.

EXPERIMENTAL SECTION

General Information. All reactions were carried out with exclusion of air using Schlenk-tube techniques or in a drybox. Pentane and toluene were obtained oxygen- and water-free from an MBraun solvent purification apparatus. ^{1}H, ^{13}C{^{1}H}, ^{31}P{^{1}H}, and ^{11}B{^{1}H} NMR spectra were recorded on Bruker 300 ARX, Bruker Avance 300 MHz, Bruker Avance 400 MHz, and Bruker Avance 500 MHz instruments. Chemical shifts (expressed in ppm) are referenced to residual solvent peaks (^{1}H, ^{13}C{^{1}H}), external 85% H_3PO_4 (^{31}P{^{1}H}), or $BF_3{\cdot}OEt_2$ (^{11}B{^{1}H}). Coupling constants *J* and *N* are given in hertz. Attenuated total reflection infrared spectra (ATR-IR) of solid samples were run on a PerkinElmer Spectrum 100 FT-IR spectrometer. C, H, and N analyses were carried out in a PerkinElmer 2400 CHNS/O analyzer. High-resolution electrospray mass spectra were acquired using a MicroTOF-Q hybrid quadrupole time-of-flight spectrometer (Bruker Daltonics, Bremen, Germany). Rh(Bpin){xant(P^{i}Pr$_2$)$_2$} (**1**) was prepared by the published method.[14]

Reaction of Rh(Bpin){xant(P^{i}Pr$_2$)$_2$} (1) with 2-Butyne: Preparation of Rh{(*Z*)-C(Me)═C(Me)Bpin}{xant(P^{i}Pr$_2$)$_2$} (2). 2-Butyne (35 *μ*L, 0.446 mmol) was added to a solution of **1** (200 mg, 0.297 mmol) in pentane (5 mL), and the resulting reddish solution was concentrated immediately to dryness to afford a red oil. Pentane was added and evaporated until a red residue was obtained. This residue was washed with the minimum of amount of pentane to afford a red solid that was dried in vacuo. Yield: 196.5 mg (91%). Anal. Calcd for $C_{37}H_{58}BO_3P_2Rh$: C, 61.17; H, 8.05. Found: C, 60.89; H, 7.73. HRMS (electrospray, *m*/*z*): calcd for $C_{37}H_{58}BO_3P_2Rh$ [M]$^+$ 725.2932; found 725.2892. IR (cm^{-1}): *ν*(C═C) 1461 (w), *ν*(C−O−C) 1029 (m). ^{1}H NMR (300.13 MHz, C_6D_6, 298 K): *δ* 7.27 (m, 2H, CH-arom), 7.03 (dd, $^{3}J_{H-H}$ = 7.7, $^{5}J_{H-P}$ = 1.6, 2H, CH-arom), 6.86 (t, $^{3}J_{H-H}$ = 7.5, 2H, CH-arom), 2.89 (s, 3H, CH_3), 2.70 (m, 2H, PC*H*(CH$_3$)$_2$), 2.45 (m, 2H, PC*H*(CH$_3$)$_2$), 2.37 (s, 3H, CH_3), 1.43 (dvt, J_{H-H} = 7.6, *N* = 15.8, 6H, PCH(C*H*$_3$)$_2$), 1.33 (dvt, $^{3}J_{H-H}$ = 7.4, *N* = 15.7, 6H, PCH(C*H*$_3$)$_2$), 1.32 (dvt, $^{3}J_{H-H}$ = 6.9, *N* = 13.8, 6H, PCH(C*H*$_3$)$_2$), 1.28 (s, 3H, CH_3 POP), 1.27 (s, 12H, CH_3 Bpin), 1.23 (s, 3H, CH_3 POP), 1.23 (dvt, $^{3}J_{H-H}$ = 6.8, *N* = 13.7, 6H, PCH(C*H*$_3$)$_2$). ^{13}C{^{1}H}-apt plus HSQC and HMBC NMR (75.47 MHz, C_7D_8, 267 K): *δ* 187.1 (dt, $^{1}J_{C-Rh}$ = 38.9, $^{2}J_{C-P}$ = 12.1, Rh−C═), 155.4 (vt, *N* = 15.8, C-arom POP), 130.7 (s, CH-arom POP), 130.5 (vt, *N* = 4.4, C-arom POP), 127.2 (s, CH-arom POP), 125.8 (vt, *N* = 14.6, C-arom POP), 123.6 (s, CH-arom POP), 118.7 (resonance inferred from the HMBC spectrum, ═*C*-Bpin), 81.2 (s, C Bpin), 34.2 (s, C(CH$_3$)$_2$), 33.9 (s, *C*(CH$_3$)$_2$), 31.2 (s, C(*C*H$_3$)$_2$), 30.9 (dvt, $^{3}J_{C-Rh}$ = 3.0, *N* = 5.6, RhC(*C*H$_3$)), 25.8 (dvt, $^{2}J_{C-Rh}$ = 2.5, *N* = 16.5, PCH(CH$_3$)$_2$), 25.3 (s, CH_3 Bpin), 24.8 (dvt, $^{2}J_{C-Rh}$ = 3.8, *N* = 16.3, PCH(CH$_3$)$_2$), 20.0 (vt, *N* = 7.8, PCH(CH$_3$)$_2$), 18.8 (vt, *N* = 8.6, PCH(CH$_3$)$_2$), 18.3 (s, PCH(CH$_3$)$_2$), 18.1 (s, PCH(CH$_3$)$_2$), 17.8 (s, ═C(CH$_3$)Bpin). ^{31}P{^{1}H} NMR (121.49 MHz, C_6D_6, 298 K): *δ* 32.8 (d, $^{1}J_{P-Rh}$ = 193.6). ^{11}B NMR (96.29 MHz, C_6D_6, 298 K): *δ* 31.2 (br).

Isomerization of Rh{(*Z*)-C(Me)═C(Me)Bpin}{xant(P^{i}Pr$_2$)$_2$} (2): Preparation of Rh{(*E*)-C(Me)═C(Me)Bpin}{xant(P^{i}Pr$_2$)$_2$} (3). A solution of **2** (100 mg, 0.138 mmol) in pentane (5 mL) was heated at 60 °C for 2 h. After this time, the red solution thus obtained was dried in vacuo, affording a red oil. Addition of pentane (0.5 mL) afforded a red solid that was washed with pentane (1 mL) and dried in vacuo. Yield: 86 mg (86%). Anal. Calcd for $C_{37}H_{58}BO_3P_2Rh$: C, 61.17; H, 8.05. Found: C, 60.96; H, 7.74. HRMS (electrospray, *m*/*z*): calcd for $C_{37}H_{58}BO_3P_2Rh$ [M]$^+$ 725.2932; found 725.2961. IR (cm^{-1}): *ν*(C═C) 1546 (w), *ν*(C−O−C) 1031 (m). ^{1}H NMR (300.13 MHz, C_6D_6, 298 K): *δ* 7.22 (m, 2H, CH-arom), 7.01 (dd, $^{3}J_{H-H}$ = 7.7, $^{5}J_{H-P}$ = 1.5, 2H, CH-arom), 6.82 (t, $^{3}J_{H-H}$ = 7.6, 2H, CH-arom), 3.32 (s, 3H, ═C(C*H*$_3$)Bpin), 3.09 (s, 3H RhC(C*H*$_3$)), 2.45 (m, 4H, PC*H*(CH$_3$)$_2$), 1.40 (dvt, $^{3}J_{H-H}$ = 8.8, *N* = 16.0, 6H, PCH(C*H*$_3$)$_2$), 1.36 (dvt, $^{3}J_{H-H}$ = 8.9, *N* = 16.1, 6H, PCH(C*H*$_3$)$_2$), 1.28 (s, 12H, *C*H$_3$ Bpin), 1.23 (s, 3H, CH_3 POP), 1.20 (dvt, $^{3}J_{H-H}$ = 7.3, *N* = 12.9, 6H, PCH(C*H*$_3$)$_2$), 1.19 (s, 3H, CH_3 POP), 1.16 (dvt, $^{3}J_{H-H}$ = 6.2, *N* = 12.9, 6H, PCH(C*H*$_3$)$_2$). ^{13}C{^{1}H}-apt plus HSQC and HMBC NMR (75.48 MHz, C_6D_6, 298 K): *δ* 194.8 (dt, $^{1}J_{C-Rh}$ = 38.3, $^{2}J_{C-P}$ = 11.0, Rh−C═), 155.3 (vt, *N* = 15.2, C-arom POP), 131.1 (s, CH-arom POP), 130.5 (vt, *N* = 4.8, C-arom POP), 127.5 (s, CH-arom POP), 125.6 (vt, *N* = 14.9, C-arom POP), 123.7 (s, CH-arom POP), 119.6 (resonance inferred from the HMBC spectrum, ═*C*-Bpin), 81.0 (s, C Bpin), 34.0 (s, *C*(CH$_3$)$_2$), 33.3, 32.9 (both s, C(*C*H$_3$)$_2$), 32.0 (dt, $^{3}J_{C-Rh}$ = 2.2, $^{4}J_{C-P}$ = 2.2, ═C(*C*H$_3$)Bpin), 28.5 (d, $^{2}J_{C-Rh}$ = 4.3, RhC(*C*H$_3$)), 25.3 (s, CH_3 Bpin), 26.0 (dvt, $^{2}J_{C-Rh}$ = 3.9, *N* = 15.9, PCH(CH$_3$)$_2$), 26.0 (dvt, $^{2}J_{C-Rh}$ = 3.8, *N* = 15.7, PCH(CH$_3$)$_2$), 19.5 (vt, *N* = 8.5, PCH(CH$_3$)$_2$), 18.7 (vt, *N* = 8.9, PCH(CH$_3$)$_2$), 18.4, 18.1 (both s, PCH(*C*H$_3$)$_2$). ^{31}P{^{1}H} NMR (121.49 MHz, C_6D_6, 298 K): *δ* 34.8 (d, $^{1}J_{P-Rh}$ = 191.0). ^{11}B NMR (128.38 MHz, C_6D_6, 298 K): *δ* 30.6 (br).

NMR Spectroscopy Study of the Isomerization of Rh{(*Z*)-C(CH$_3$)═C(CH$_3$)Bpin}{xant(P^{i}Pr$_2$)$_2$} (2) into Rh{(*E*)-C(CH$_3$)═C(CH$_3$)Bpin}{xant(P^{i}Pr$_2$)$_2$} (3). The experimental procedure is described for a particular case, but the same method was used in all experiments, which were run in duplicate. In the glovebox, an NMR tube was charged with a solution of **2** (10 mg, 0.014 mmol) in toluene-d_8 (0.42 mL), and a capillary tube filled with a solution of the internal standard (PCy_3) in toluene-d_8 was placed in the NMR tube. The tube was immediately introduced into an NMR probe preheated at the desired temperature, and the reaction was monitored by ^{31}P{^{1}H} NMR at different intervals of time. Rate constants were obtained by plotting eq 1.

NMR Spectroscopic Study of the Reaction of Rh{(*E*)-C(CH$_3$)═C(CH$_3$)Bpin}{xant(P^{i}Pr$_2$)$_2$} (3) with B$_2$pin$_2$. *Determina-*

DOI: 10.1021/acs.organomet.8b00259
Organometallics XXXX, XXX, XXX−XXX

tion of the Reaction Order for B_2pin_2. The experimental procedure is analogous to that described for the isomerization of **2** into **3**, starting from **3** (10 mg, 0.014 mmol, 0.035 M) and variable concentrations of B_2pin_2 (from 1.64 to 2.95 M) in toluene-d_8 (0.42 mL). The experiments were carried out at 333 K.

Determination of k_3. The experimental procedure is analogous to that described for the isomerization of **2** into **3**, starting from **3** (10 mg, 0.014 mmol) and B_2pin_2 (245 mg, 1 mmol, 2.30 M) in toluene-d_8 (0.42 mL).

The ^{1}H NMR spectra recorded after the reaction of **3** with B_2pin_2 shows the presence of (*E*)-pinBC(Me)=C(Me)Bpin, along with peaks assigned to B_2pin_2 and **1**. Spectroscopic data of (*E*)-pinBC(Me)=C(Me)Bpin are as follows. ^{1}H NMR (300.13 MHz, C_7D_8, 298 K): δ 2.39 (s, 6H, =C−CH_3), 1.05 (s, 24H, CH_3 Bpin). ^{13}C{^{1}H}-apt plus HSQC and HMBC NMR (75.47 MHz, C_7D_8, 298 K): δ 82.8 (s, C Bpin), 24.8 (s, CH_3 Bpin), 21.1 (s, CH_3). ^{11}B NMR (96.29 MHz, C_7D_8, 298 K): δ 30.7 (s).

NMR Spectroscopic Study of the reaction of Rh{(*Z*)-C(CH$_3$)=C(CH$_3$)Bpin}{xant(P^{i}Pr$_2$)$_2$} (2) with B_2pin_2. The experimental procedure is analogous to that described for the isomerization of **2** into **3**, starting from **2** (10 mg, 0.014 mmol) and B_2pin_2 (253 mg, 1 mmol, 2.45 M) in toluene-d_8 (0.42 mL). With this experiment we can calculate rate constants k_1 (from eq 1), and k_3 (from eq 7, by least-squares adjustment).

Borylation of 2-Butyne with B_2pin_2 Catalyzed by Rh(Bpin){xant(P^{i}Pr$_2$)$_2$} (1). In an argon-filled glovebox, an Ace pressure tube was charged with **1** (10 mg, 0.015 mmol), B_2pin_2 (75.5 mg, 0.3 mmol), 2-butyne (23.5 μL, 0.3 mmol), and 5 mL of *n*-octane. The resulting mixture was stirred at 70 °C for 24 h. After this time, the solvent was evaporated under reduced pressure to afford a crude reaction mixture. After purification of the crude reaction mixture by flash chromatography over Florisil using *n*-pentane as eluent, (*Z*)-pinBC(Me)=C(Me)Bpin was isolated in 68% yield (75% crude yield). ^{1}H NMR (300.13 MHz, C_7D_8, 298 K): δ 1.88 (s, 6H, =CCH_3), 1.15 (s, 24H, CH_3 Bpin). ^{13}C{^{1}H}-apt plus HSQC and HMBC NMR (75.47 MHz, C_7D_8, 298 K): δ 155.8 (resonance inferred from the HMBC spectrum, =C−Bpin), 83.4 (s, C Bpin), 25.4 (s, CH_3 Bpin), 17.1 (s, =CCH_3). ^{11}B NMR (96.29 MHz, C_7D_8, 298 K): δ 30.6 (s).

Reaction of Rh(Bpin){xant(P^{i}Pr$_2$)$_2$} (1) with B_2cat_2. B_2cat_2 (10.6 mg, 0.045 mmol) was added to a solution of **1** (15 mg, 0.022 mmol) in toluene-d_8 (0.4 mL) placed in an NMR tube. The ^{31}P{^{1}H} NMR spectrum recorded after 5 min at room temperature shows a doublet at 54.5 ppm ($^1J_{P-Rh}$ = 159.9 Hz) assigned to Rh(Bcat){xant(P^{i}Pr$_2$)$_2$} and a broad doublet at 31.5 ppm ($^1J_{P-Rh}$ = 78.1 Hz) that was assigned to Rh(Bpin)(Bcat)$_2${xant(P^{i}Pr$_2$)$_2$}. ^{11}B{^{1}H} NMR (96.29 MHz, C_7D_8, 298 K): δ 48.8 (very br, Rh(Bcat){xant(P^{i}Pr$_2$)$_2$}), 31.2 (br, pinB-Bcat).

■ ASSOCIATED CONTENT

Supporting Information

The Supporting Information is available free of charge on the ACS Publications website at DOI: 10.1021/acs.organomet.8b00259.

Determination of the ^{31}P relaxation times, plot of ln(d[**3**]/dt) vs ln[B_2pin_2], structural analysis of complexes **2**, **3**, and (*Z*)-pinBC(Me)=C(Me)Bpin, computational details and energies of calculated complexes, and NMR spectra (PDF)

Cartesian coordinates of the optimized structures (XYZ)

Accession Codes

CCDC 1832730−1832732 contain the supplementary crystallographic data for this paper. These data can be obtained free of charge via www.ccdc.cam.ac.uk/data_request/cif, or by emailing data_request@ccdc.cam.ac.uk, or by contacting The Cambridge Crystallographic Data Centre, 12 Union Road, Cambridge CB2 1EZ, UK; fax: +44 1223 336033.

■ AUTHOR INFORMATION

Corresponding Author

*E-mail for M.A.E.: maester@unizar.es.

ORCID

Miguel A. Esteruelas: 0000-0002-4829-7590

Montserrat Oliván: 0000-0003-0381-0917

Enrique Oñate: 0000-0003-2094-719X

Notes

The authors declare no competing financial interest.

■ ACKNOWLEDGMENTS

Financial support from the MINECO of Spain (Projects CTQ2017-82935-P and Red de Excelencia Consolider CTQ2016-81797-REDC), the Diputación General de Aragón (E06_17R), FEDER, and the European Social Fund is acknowledged.

■ REFERENCES

(1) Planells, M.; McCulloch, I.; Donaghey, J. E.; Martin, R. Small molecule heteroacenes as semiconductors. WO2015/097078 A2, 2015.

(2) Mishra, A. K.; Vaidyanathan, S.; Noguchi, H.; Doetz, F.; Zu, B.; Basuki, J. S. Semiconductor materials prepared from bridged bithiazole copolymers, US2013/0144065 A1, 2013.

(3) (a) Takaya, J.; Iwasawa, N. *ACS Catal.* **2012**, *2*, 1993−2006. (b) Alfaro, R.; Parra, A.; Alemán, J.; Tortosa, M. *Synlett* **2013**, *24*, 804−812. (c) Yoshida, H. *ACS Catal.* **2016**, *6*, 1799−1811. (d) Ansell, M. B.; Navarro, O.; Spencer, J. *Coord. Chem. Rev.* **2017**, *336*, 54−77.

(4) Nakagawa, N.; Hatakeyama, T.; Nakamura, M. *Chem. - Eur. J.* **2015**, *21*, 4257−4261.

(5) (a) Adams, C. J.; Baber, R. A.; Batsanov, A. S.; Bramham, G.; Charmant, J. P. H.; Haddow, M. F.; Howard, J. A. K.; Lam, W. H.; Lin, Z.; Marder, T. B.; Norman, N. C.; Orpen, A. G. *Dalton Trans.* **2006**, 1370−1373. (b) Ferrand, L.; Lyu, Y.; Rivera-Hernández, A.; Fallon, B. J.; Amatore, M.; Aubert, C.; Petit, M. *Synthesis* **2017**, *49*, 3895−3904.

(6) Iwadate, N.; Suginome, M. *J. Am. Chem. Soc.* **2010**, *132*, 2548−2549.

(7) Ansell, M. B.; Menezes da Silva, V. H.; Heerdt, G.; Braga, A. A. C.; Spencer, J.; Navarro, O. *Catal. Sci. Technol.* **2016**, *6*, 7461−7467.

(8) For selected relevant examples see: (a) Ishiyama, T.; Matsuda, N.; Miyaura, N.; Suzuki, A. *J. Am. Chem. Soc.* **1993**, *115*, 11018−11019. (b) Ishiyama, T.; Matsuda, N.; Murata, M.; Ozawa, F.; Suzuki, A.; Miyaura, N. *Organometallics* **1996**, *15*, 713−720. (c) Thomas, R. Ll.; Souza, F. E. S.; Marder, T. B. *J. Chem. Soc., Dalton Trans.* **2001**, 1650−1656. (d) Ali, H. A.; Quntar, A. E. A. A.; Goldberg, I.; Srebnik, M. *Organometallics* **2002**, *21*, 4533−4539. (e) Lillo, V.; Mata, J.; Ramírez, J.; Peris, E.; Fernandez, E. *Organometallics* **2006**, *25*, 5829−5831. (f) Grirrane, A.; Corma, A.; García, H. *Chem. - Eur. J.* **2011**, *17*, 2467−2478. (g) Mora-Radó, H.; Bialy, L.; Czechtizky, W.; Méndez, M.; Harrity, J. P. A. *Angew. Chem., Int. Ed.* **2016**, *55*, 5834−5836.

(9) Lillo, V.; Fructos, M. R.; Ramírez, J.; Braga, A. A. C.; Maseras, F.; Díaz-Requejo, M. M.; Pérez, P. J.; Fernández, E. *Chem. - Eur. J.* **2007**, *13*, 2614−2621.

(10) Chen, Q.; Zhao, J.; Ishikawa, Y.; Asao, N.; Yamamoto, Y.; Jin, T. *Org. Lett.* **2013**, *15*, 5766−5769.

(11) (a) Nagashima, Y.; Hirano, K.; Takita, R.; Uchiyama, M. *J. Am. Chem. Soc.* **2014**, *136*, 8532−8535. (b) Nagao, K.; Ohmiya, H.; Sawamura, M. *Org. Lett.* **2015**, *17*, 1304−1307.

(12) Obligacion, J. V.; Neely, J. M.; Yazdani, A. N.; Pappas, I.; Chirik, P. J. *J. Am. Chem. Soc.* **2015**, *137*, 5855−5858.

(13) (a) Onozawa, S.; Tanaka, M. *Organometallics* **2001**, *20*, 2956−2958. (b) Zhang, L.; Cheng, J.; Carry, B.; Hou, Z. *J. Am. Chem. Soc.* **2012**, *134*, 14314−14317.

(14) Esteruelas, M. A.; Oliván, M.; Vélez, A. *Organometallics* **2015**, *34*, 1911−1924.

DOI: 10.1021/acs.organomet.8b00259
Organometallics XXXX, XXX, XXX−XXX

(15) (a) Esteruelas, M. A.; Oliván, M.; Vélez, A. *Inorg. Chem.* **2013**, *52*, 5339−5349. (b) Haibach, M. C.; Wang, D. Y.; Emge, T. J.; Krogh-Jespersen, K.; Goldman, A. S. *Chem. Sci.* **2013**, *4*, 3683−3692. (c) Esteruelas, M. A.; Oliván, M.; Vélez, A. *Inorg. Chem.* **2013**, *52*, 12108−12119.
(16) See for example: (a) Braun, T.; Noveski, D.; Neumann, B.; Stammler, H.-G. *Angew. Chem., Int. Ed.* **2002**, *41*, 2745−2748. (b) Itazaki, M.; Yoda, C.; Nishihara, Y.; Osakada, K. *Organometallics* **2004**, *23*, 5402−5409. (c) Kumazawa, S.; Rodriguez Castanon, J.; Onishi, N.; Kuwata, K.; Shiotsuki, M.; Sanda, F. *Organometallics* **2012**, *31*, 6834−6842. (d) Onishi, N.; Shiotsuki, M.; Masuda, T.; Sano, N.; Sanda, F. *Organometallics* **2013**, *32*, 846−853.
(17) Esteruelas, M. A.; Oliván, M.; Vélez, A. *J. Am. Chem. Soc.* **2015**, *137*, 12321−12329.
(18) See for example: (a) Chung, L. W.; Wu, Y.-D.; Trost, B. M.; Ball, Z. T. *J. Am. Chem. Soc.* **2003**, *125*, 11578−11582. (b) Trost, B. M.; Ball, Z. T. *J. Am. Chem. Soc.* **2005**, *127*, 17644−17655. (c) Pawley, R. J.; Huertos, M. A.; Lloyd-Jones, G. C.; Weller, A. S.; Willis, M. C. *Organometallics* **2012**, *31*, 5650−5659. (d) Ding, S.; Song, L.-J.; Chung, L. W.; Zhang, X.; Sun, J.; Wu, Y.-D. *J. Am. Chem. Soc.* **2013**, *135*, 13835−13842. (e) Pérez-Torrente, J. J.; Nguyen, D. H.; Jiménez, M. V.; Modrego, F. J.; Puerta-Oteo, R.; Gómez-Bautista, D.; Iglesias, M.; Oro, L. A. *Organometallics* **2016**, *35*, 2410−2422. (f) Teo, W. J.; Wang, C.; Tan, Y. W.; Ge, S. *Angew. Chem., Int. Ed.* **2017**, *56*, 4328−4332.
(19) Tanke, R. S.; Crabtree, R. H. *J. Am. Chem. Soc.* **1990**, *112*, 7984−7989.
(20) Ojima, I.; Clos, N.; Donovan, R. J.; Ingallina, P. *Organometallics* **1990**, *9*, 3127−3133.
(21) (a) Alós, J.; Bolaño, T.; Esteruelas, M. A.; Oliván, M.; Oñate, E.; Valencia, M. *Inorg. Chem.* **2013**, *52*, 6199−6213. (b) Esteruelas, M. A.; Nolis, P.; Oliván, M.; Oñate, E.; Vallribera, A.; Vélez, A. *Inorg. Chem.* **2016**, *55*, 7176−7181. (c) Esteruelas, M. A.; García-Yebra, C.; Martín, J.; Oñate, E. *Inorg. Chem.* **2017**, *56*, 676−683. (d) Karmel, C.; Li, B.; Hartwig, J. F. *J. Am. Chem. Soc.* **2018**, *140*, 1460−1470.
(22) See for example: (a) Johnson, H. C.; McMullin, C. L.; Pike, S. D.; Macgregor, S. A.; Weller, A. S. *Angew. Chem., Int. Ed.* **2013**, *52*, 9776−9780. (b) Johnson, H. C.; Leitao, E. M.; Whittell, G. R.; Manners, I.; Lloyd-Jones, G. C.; Weller, A. S. *J. Am. Chem. Soc.* **2014**, *136*, 9078−9093. (c) Adams, G. M.; Weller, A. S. *Coord. Chem. Rev.* **2018**, *355*, 150−172. (d) Adams, G. M.; Colebatch, A. L.; Skornia, J. T.; McKay, A. I.; Johnson, H. C.; Lloyd-Jones, G. C.; Macgregor, S. A.; Beattie, N. A.; Weller, A. S. *J. Am. Chem. Soc.* **2018**, *140*, 1481−1495.
(23) Perutz, R. N.; Sabo-Etienne, S. *Angew. Chem., Int. Ed.* **2007**, *46*, 2578−2592.
(24) Connors, K. A. *Chemical Kinetics: The Study of Reaction Rates in Solution*; Wiley-VCH, 1990.
(25) (a) Lesley, M. J. G.; Norman, N. C.; Orpen, A. G.; Starbuck, J. *New J. Chem.* **2000**, *24*, 115−117. (b) Oschmann, W.; Borner, C.; Kleeberg, C. *Dalton Trans.* **2018**, *47*, 5318−5327.
(26) Esteruelas, M. A.; López, A. M.; Mora, M.; Oñate, E. *Organometallics* **2015**, *34*, 941−946.
(27) Werner, H. *Angew. Chem., Int. Ed. Engl.* **1983**, *22*, 927−949.

DOI: 10.1021/acs.organomet.8b00259
Organometallics XXXX, XXX, XXX−XXX